DATA ACQUISITION AND ANALYSIS FOR ADVANCED DIGITAL IONOSONDES

J. W. Wright[1], M. L. V. Pitteway[2], M. T. Rietveld[3], Robert C. Livingston[4]

[1]NGDC/NOAA and CIRES, Boulder CO, USA. bill.wright@noaa.gov

[2]Brunel University Uxbridge, UK. Email: Mike.Pitteway@brunel.ac.uk

[3]EISCAT Scientific Association, Tromsø Norway. Email: mike.rietveld@eiscat.uit.no

[4] Scion Associates, WA. Email: livingston@scion-associates.com

ABSTRACT

The modern ionosonde, if it follows established 'Dynasonde' precedents, is a precision instrument for research, space weather and environmental monitoring. Noise is discriminated from genuine echo data, which is uniquely defined in terms of physical parameters (3D echolocation, Doppler, polarization), each with attached error estimates. Further analyses of these parameters yield the electron-density distribution, quantitative evidence of auroral precipitation, vector velocities, deterministic identification of AGWs, and spectral parameters ($\Delta N/N$, power-law index, anisotropy) of ionospheric irregularities in the 0.1 to 1000 km scale range. Standard (e.g. foE, fof2) and non-standard (TEC, spread F) parameters are estimated each several minutes and with real-time capability.

INTRODUCTION

At medium and high frequencies, radio waves are reflected totally from the ionosphere by unique ionization densities. Echoes have very large Signal/Noise margins provided that adequate (1 - 10 kW) radar peak powers are used. Nevertheless, natural and man-made sources contribute false echoes (lightning, electrostatic noise, vehicle ignition, modulated broadcast transmissions, etc.). In classical analog ionosondes, no attempt was made to recognize and reject such noise, instead relying on expert recognition of characteristic patterns in the echo-delay vs. radio-frequency domain. We discuss in this paper an echo recognition, parameterization and data analysis system integrated as within the layout of Figure 1. It is applicable for dynasonde instruments at present, and could typify the information returned by the world's loosely coordinated 'network' of some 120 monitoring ionosondes, if appropriate hardware upgrades were made.

Modern ionosondes digitally sample the receiver-output complex-amplitude at short (e.g. 10 *ms*) time intervals between about 60 and 800km of range delay, whether or not echoes are present there. In the dynasonde, echoes are defined from a set of 4 to 8 transmitted pulses (a 'pulset'), representing a very carefully planned exercise in experimental design. Within the set, different receiving antennas are assigned to each system receiver, and small radio-frequency offsets are applied. Receiving dipole antennas are spatially separated and oriented as part of the experiment design. Each retained complex amplitude provides an amplitude-modulus and phase angle, characteristic of the antenna, its orientation, the time, and the precise radio frequency of its corresponding transmitted pulse.

ECHO RECOGNITION AND PARAMETERIZATION

Let us consider the physical meaning of phase *differences* $\Delta\phi$ within a pulset:

a) phase differences $\Delta\phi/\Delta t$ among pulses of exactly the same radio frequency and same receiving antenna, sample an echo time dependence or "Doppler".

b) phase differences $\Delta\phi/\Delta y$, ($\Delta\phi/\Delta x$) among antennas separated along North-South (East-West) baselines at the same time and precise radio frequency, sample components of the spatial orientation of the echo wavefront, thus defining the direction-of-arrival, or 'echolocation'. Some pulset designs permit estimation of wavefront 'curvatures', $\Delta^2\phi/\Delta y^2$, ($\Delta^2\phi/\Delta x^2$).

c) phase differences $\Delta\phi/\Delta f$ between pulses of slightly different radio frequency, (necessarily at different times!) define the echo range delay according to the "principle of stationary phase". Note that by the mean value theorem, the group range defined by this difference quotient is assured to exist somewhere in the interval Δf (~ 8 kHz, typically small compared to the pulse bandwidth, ~30 kHz in the dynasonde). Some pulset designs permit estimation of $\Delta^2\phi/\Delta f^2$.

d) phase differences between antennas of different (e.g. orthogonal) azimuth, contain a large (typically +90º or -90º) contribution (echo 'chirality') arising from the (left or right-hand) nearly circular polarization of ionospheric echoes.

In addition to these 5 differences, the simple average phase among members of the set has many downstream uses. Thus, we have at least six independent parameters defined from at least 8 (and, for 8-pulse sets with two receivers, 16) echo phase measurements. Overdetermination by least-squares yields error estimates on each parameter. Future instruments will have one receiver for each antenna; this simplifies experiment design, reducing errors and phase ambiguities. In a recent development [1] the data transformations of (a) – (d) not only define the basic echo attributes, but also are the basis for echo recognition and impulsive-noise rejection.

FURTHER ANALYSES FOR SPACE WEATHER AND TELECOMMUNICATIONS.

DSND is a continuously evolving analysis environment for dynasonde data. The most important analyses for general-purpose ionospheric applications comprise a specific sequence of steps, which proceed automatically; these steps are described below.

(1) By the echo recognition and parameterization steps above, each echo is now described by two independent variables (radio frequency f, time t), seven phase-dependent attributes (XL, YL east, north echolocations; R', group range; V*, line-of-sight Doppler; PP, polarization chirality; R*, mean phase; EP, phase-error), and one (peak) amplitude.

(2) Echoes are classified into 'traces' [2]: A formal process organizes echo pairs which are similar (within chosen tolerances) according to the 10 attributes listed in (1). Each 'new' member of a pair inherits as 'children' all of the members of the class to which the 'old' member belongs. Because of this list progression, the local values of each echo attribute can change slowly along the independent variables of the trace. An ionogram recording containing typically >2000 echoes may be organized into typically <10 traces. Colors in the ionogram example of Figure 1 distinguish individual traces (colors are re-used here, without significance).

(3) Useful trace properties are established: average coordinates and new attributes (mean f, mean R', $\Delta R'/\Delta f$, etc.) are obtained at the ends of each trace; also trace midpoint mean f, R' are obtained. If $|\Delta R'/\Delta f| > 100$ km/MHz at either end of a trace, two values of $(\Delta R'/\Delta f)^{-1}$ near that end are extrapolated (*vs* f) to zero, thus defining systematically the layer peak penetration frequencies. This procedure is exactly valid [3] for radiowave penetration of a parabolic layer peak in absence of magnetoionic effects..

(4) Trace *pairs* are compared by theoretically based, polarization-dependent shifts to common plasma frequency, and empirical group-range differences are used to establish which Z, O, X traces represent the *same* ionospheric structures. ('Z' traces are only sought at high latitudes where magnetic dip > 65°).

(5) Trace *pairs* are compared to establish E, F –region transitions. Trace pairs of unlike polarization are ignored for this. Penetration values from (3) are used, if available, and the comparison thereby determines fzE, foE, and fxE.

(6) Similarly, the largest F-region penetrations establish fzF2, foF2, fxF2.

(7) Trace *pairs* are compared to establish 'Multiple-echo' traces, i.e., those in which echoes have experienced one or more ground reflections.

(8) Traces in the vicinity of layer penetrations are analyzed for 'Spread Echo' quantification [4]. This analysis yields a mean penetration frequency and standard-deviation expressing the 'spread width', $\Delta f/f$; theory suggests that $\Delta f/f$ is an estimate of $\Delta N/N$ at the layer peak, relevant to irregularity scales larger than the radio first Fresnel diameter, thus >10 km.

These eight steps represent a nearly complete organization of the ionogram echoes into traces, and of the traces into broad ionospheric structures. As mentioned, several standard ionospheric parameters are determined while these steps are underway. Subsequent steps apply a series of major analysis subsystems to the traces and their constituent echo parameters:

(9) Traces are selected for N(h) inversion, using (at present) the 'POLAN' method. Trace selection seeks to use traces from near the zenith if alternatives are available. O and X trace information is supplied to POLAN for nighttime underlying ionization (night E) starting-height corrections, and for E-F valley corrections. POLAN fits a Chapman function at layer peaks [5] to obtain the standard parameters hmaxE, hmaxF, the respective layer thicknesses or scale heights, a plausible valley shape, and an extrapolation above hmaxF. An estimate of ionospheric total electron content (TEC) is obtained from the N(h) profile plus its topside Chapman extrapolation.

(10) Ionospheric vector velocities are calculated for each trace independently. The method combines echo line-of-sight Doppler with echolocation in a least-squares process [6]. In the F-region the results may describe the electric field, or winds, or their combined effect; winds and turbulence usually dominate in the E-region.

(11) 'Phase structure function' analysis is performed [7], by which an estimate is made of the amplitude $(\Delta N/N)_{rms}$, and spectral index ν of mid-scale (0.1 – 10 km) irregularities. The analysis is applied to each trace independently, and weighted mean values are obtained to characterize the E and F regions.

It is worthwhile to note that the structure function analysis of item (11) requires information from most of the ten foregoing steps; for example, the vector velocities of item (10) permit translation from temporal to spatial irregularity scales. Furthermore, structure functions exploit the full raw-data and parameter resolution available by the dynasonde's hardware design.

CONCLUSIONS

The compact integration of modern ionosonde diagnostic capability with its applications for the geophysics, space weather and telecommunication communities is suggested by the layout of Figure 1. The ionogram image, familiar to a diminishing fraction of these communities, and symbolized as the data source in Figure 1, is itself merely another optional (and generally inessential) byproduct of the data. The primary products of the lower half of the figure are meaningful to geophysicists, modelers, and operational clients, who need not develop deep familiarity with ionosonde technology.

Not well represented by the diagram are many ways in which self-consistency can be tested in stand-alone studies. For example, eddy mixing, and F-region ionization balance (as expressed in a 'Sunrise Index' [8]), should prove to be related through diurnal and seasonal variations of the $[O]/[N_2]$ boundary condition near the turbopause. Another important example arises from the increasing capability for plasma irregularity diagnostics [7]: Large-scale gradients and plasma-contour tilts are easily measured within the 'all-sky' view of the ionosonde; together with vector velocities, the growth rate of important instabilities [9] can be estimated and tested against the estimated irregularity spectral parameters.

The capabilities shown in the figure are fully realized at present for data from only a very few dynasonde examples (at EISCAT, Tromsø Norway; Bear Lake Observatory, Utah State University; Halley Bay, British Antarctic Survey; and, most recently, Lycksele, Swedish Institute of Space Physics). Meanwhile, there are about 120 monitoring ionosondes in routine operation, which return only a small fraction of the potentially available information [10]. An upgrade of this de-facto 'network' is technologically practical and deserves the support and encouragement of URSI.

REFERENCES

[1] Wright, J. W. and M. L. V. Pitteway, A new data acquisition concept for digital ionosondes: Phase-based echo recognition and real-time parameter estimation. *Radio Science 34*, 871 - 882, 1999.

[2] Wright, J. W. and M. L. V. Pitteway, Data acquisition and analysis for research ionosondes. In *Computer Aided Processing of Ionograms and Ionosonde Records*, Proc. Session G5 at the XXVth General Assembly of URSI, Lille, France, Aug.28 - Sept. 5, 1996. Ed. by Phil Wilkinson. Report UAG 105, NGDC, NOAA, 325 Broadway, Boulder CO 80303 USA. 1998

[3] Paul, A.K. and D.L. Mackison, Scaling of the F-layer critical frequency from digital ionograms applied to observations during the solar eclipse on 26 February 1979, *J. Atmos. Terr. Phys., 43*, 221-224, 1981.

[4] Wright, J. W. Quantifying ionogram spread F. Submitted to *Adv. Space Res.* 2002 (IRI Workshop, 2001).

[5] Wright, J.W. Comment on models of the ionosphere above hmaxF2, *J. Geophys. Res. 65*, 2595-2596, 1960

[6] Wright, J.W. and M.L.V. Pitteway, High-resolution vector velocity determinations from the dynasonde. *J. Atmos. Terr. Phys. 56*, 961 - 977, 1994.

[7] Zabotin, N. A. and J. W. Wright, Ionospheric irregularity diagnostics from the phase structure functions of MF / HF radio echoes. *Radio Sci.* **36**, 757 – 771, 2001

[8] Wright, J. W. and R. O. Conkright, Prospects for an ionospheric index of neutral thermospheric composition, with space-weather applications. *J. Geophys. Res. 106*, 21063 - 21075, Oct. 2001.

[9] Hamza, A.M., Perkins instability revisited. *J. Geophys. Res. 104*, 22567-22575, 1999.

[10] Wright, J. W. and T. Bullett, The applicability of advanced ionosondes to the IRI. Submitted to *Adv. Space Res.* 2002 (IRI Workshop, 2001).

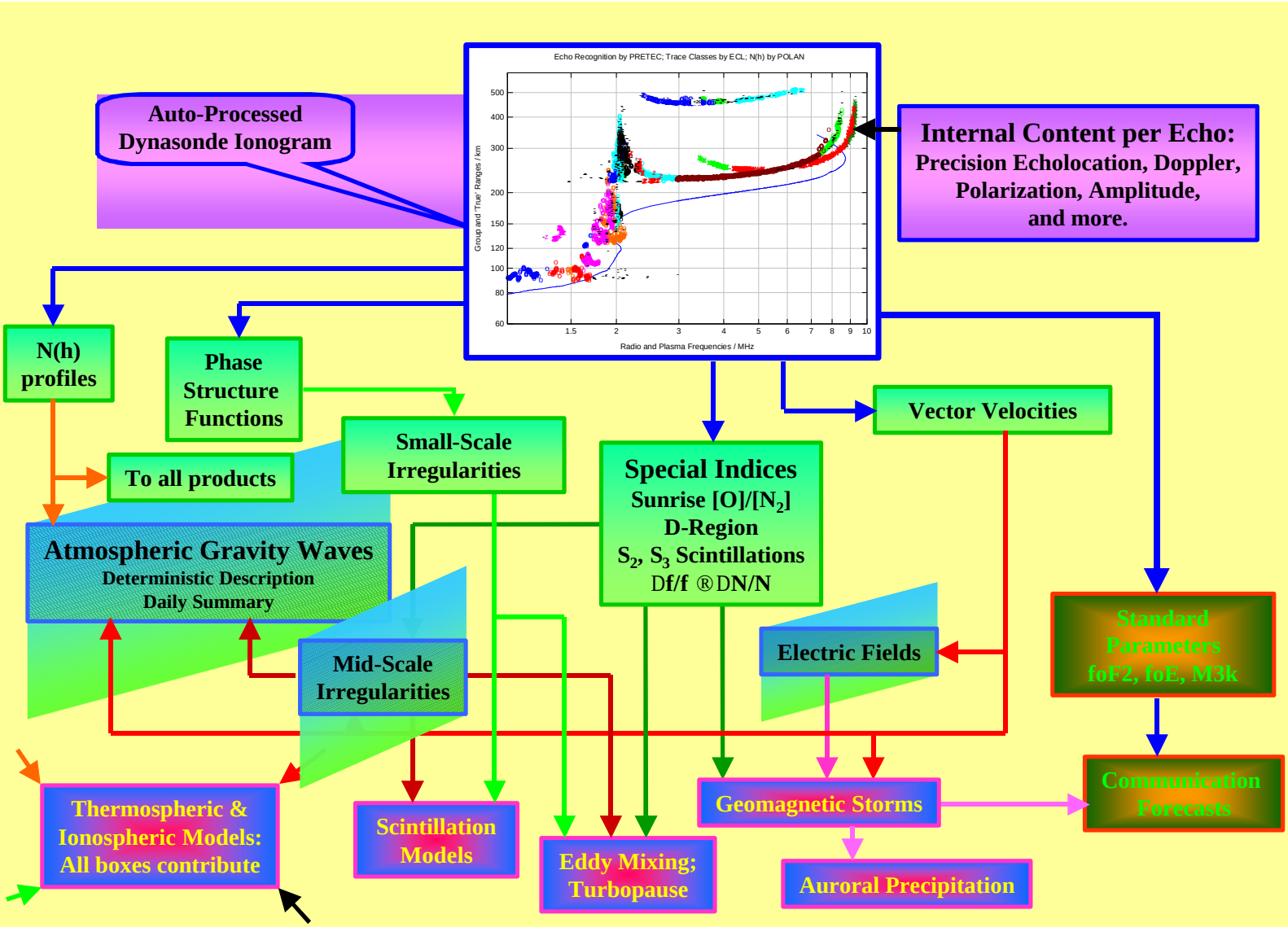

Fig. 1 Information available from advanced ionosondes. The 'ionogram image' is incidental to the quantitative products. Note multiplicity, even redundancy, of contributions to products.